Journal of Statistical Physics, Vol. 93, Nos. 3/4, 1998

Energies of a Kinked Crack Line

M. Marder[1]

This article finds the energy of slightly kinked crack fronts in order to find the rate at which thermal fluctuations cause cracks to creep in three-dimensional settings.

KEY WORDS: Fracture; creep; kinks; thermal fluctuations; energy barriers.

1. INTRODUCTION

A singularity can cut through seemingly impenetrable regions, leaving open space behind. The space Leo Kadanoff gave me was the opportunity to begin studying fracture in the spirit of moving interface problems[1] during two years in Chicago. This article will discuss some new statistical features of the problem, motivated in part by recent experiments and computer simulations.

There is a number of pieces of previous work leading into these calculations. The first is the discovery of lattice trapping by Thomson.[2, 3] A crack in a two-dimensional crystal can be trapped at a given location for a range of externally applied stresses. When external stresses place the crack at the Griffith point, the net energy required for it to progress by one lattice spacing is zero. In order to move ahead, however, the bond ahead of the crack has to be raised above the breaking point, requiring temporary addition of extra energy, which then is recovered as atoms throughout the system relax to their final configuration. One might estimate that the height of the lattice trapping energy barriers should be comparable to energies involved in snapping bonds. These energies are in turn comparable to the energy of melting, leading to the prediction that cracks should only be able

[1] Department of Physics and Center for Nonlinear Dynamics, University of Texas at Austin, Austin, Texas 78712.

0022-4715/98/1100-0511$15.00/0

to creep quickly past the energy barriers that bind them near the melting temperature.

This estimate is rather hasty, and it has long been recognized that the way in which a crack creeps actually involves a complicated progression of kinks moving along the crack surface.[4] Crack creep therefore requires a study of the energetics of kink motion. Kinks have been studied numerically,[5] some statistical consequences of having many of them have been worked out,[6] they have been modeled by a population of dislocations,[7] as continuum excitations[8] and finally have been treated in atomistic models of increasing complexity.[9–12] The calculations of ref. 12 are particularly similar to the calculations in this paper, but do not proceed in quite the way needed to answer some questions that have recently arisen in molecular dynamics simulations and experiments.

A brief summary of the new findings is as follows:

1. Lattice trapping has interesting implications for crack dynamics. In a crystal at temperature $T=0$ cracks should be incapable of steady motion at any velocity v between 0 and a lower critical value on the order of 20% of the Rayleigh wave speed. For a crack in silicon opening a (111) plane along $[1\bar{1}0]$ the minimum allowed velocity is predicted to be 1500 m/s.[13] This phenomenon can be referred to as a velocity gap.[14]

2. J. Hauch has been fracturing silicon along precisely this plane in the laboratory. The experiments are still in a preliminary stage, but seem to indicate that crack motion at any speed between 0 and 1500 m/s is possible. These experiments are at room temperature.

3. D. Holland has performed molecular dynamics simulations of cracks along this plane at a sequence of increasing temperatures. The velocity gap vanishes at a temperature of around 150 K.

A tentative conclusion to draw from these observations is that thermal fluctuations on the order of 150 K are adequate to alter completely the dynamics of low-velocity cracks in silicon. The question to settle is how this claim can be true if the relevant energy barriers are on the order of the melting temperature of 1683 K. The answer I will propose is that one cannot afford to be hasty in estimating the energy barriers a crack actually faces. When the geometry by which the crack moves forward is properly taken into account, the barriers are greatly reduced. Just as a two-dimensional crack in a three-dimensional body provides a particularly efficient way to sever the object, so a one-dimensional crack traveling along the edge of a two-dimensional crack front provides a particularly efficient way for the crack to advance. Figure 1 shows the geometry of crack motion.

A general framework has previously been worked out to study thermally-driven transitions in Hamiltonian systems, and applied to a one-dimensional model of a crack.[15] According to this formalism, transitions can be of two types.

The first type is described by transition-state theory. In this framework, the system begins in an initial state, moves upwards in energy to a transition state, and finally descends to a final state. The transition state needs to have three properties:

1. The transition state is a stationary solution of the equations of motion. All atoms are in equilibrium, typically, an unstable equilibrium. Call the energy of this configuration E_s.

2. There exists a path through configuration space where the energy of the system constantly diminishes that takes it from the transition state to the initial state.

3. Similarly, there exists a path through configuration space where the energy of the system constantly diminishes that takes it from the transition state to the final state.

If the energy of the initial state is E_i, then in this approximation the probability of moving from initial to final states is proportional to

$$e^{[E_s - E_i]/k_B T} \tag{1}$$

According to the general formalism of ref. 15, it is possible to have transitions between initial and final states that simply do not fit within this framework, particularly when the final state is something dynamical like a running crack, rather than static. It is extremely likely that thermal creep of cracks is of this type for a certain range of loading. However, in view of the complications involved just in following through the possibilities afforded by transition state theory, I will ignore this possibility here, and will focus simply upon finding the minimal set of energy barriers a crack must surmount in moving from top to bottom in Fig. 1. Rather than moving immediately to elaborate atomic interactions of the sort employed in molecular dynamics simulations,[13] I will focus upon a simple model where everything can be worked out by hand. The results suggest the sorts of possibilities that will have to be considered in more realistic settings.

Most of this paper will be devoted to explaining details of the calculations, but the end results are fairly simple, and can be displayed even before the model is described in detail. The variable Δ is a dimensionless control parameter that characterizes how hard a crack is being pulled. It equals 1 when the system has been strained just enough to make crack motion energetically possible, and increases beyond 1 as the system is strained

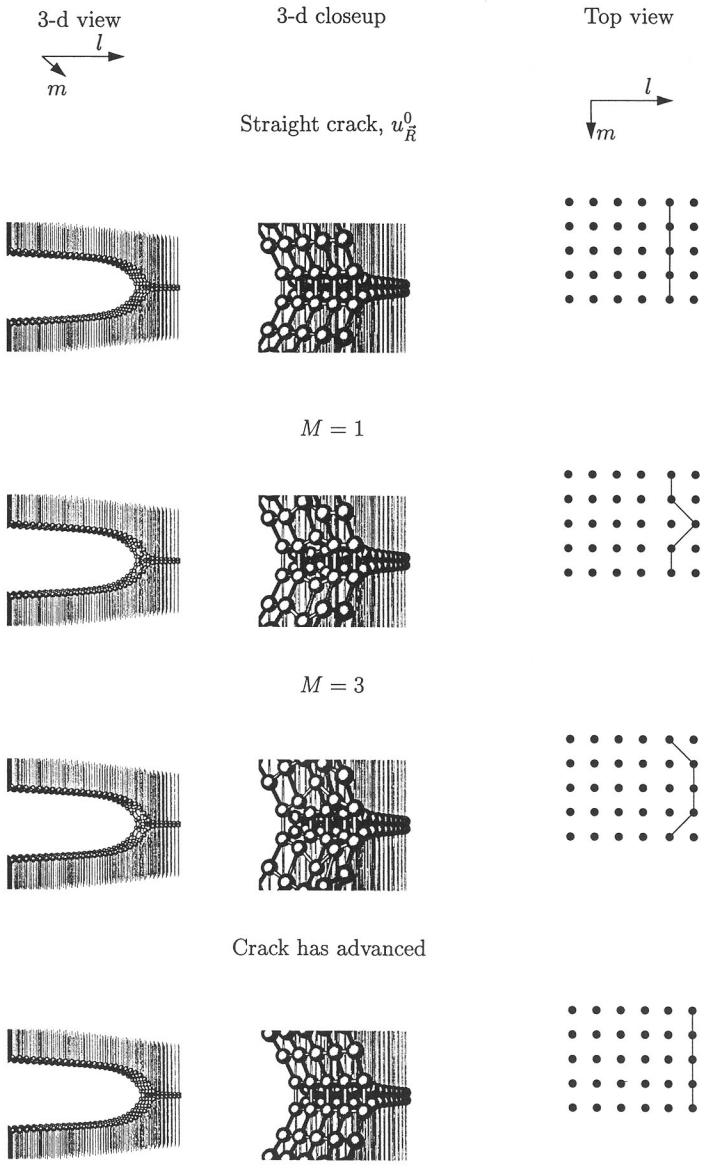

Fig. 1. Geometry of crack motion, showing a crack moving forward by one lattice spacing through the spreading of a kink. On the left are three-dimensional images of kinks of various lengths, in the center a close-up view of the broken bonds, while on the right is a schematic view of the crack front as seen from above.

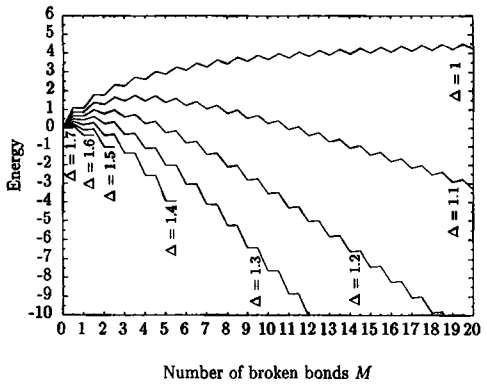

Fig. 2. Energy of kink configurations as a function of number M of broken bonds, for various values of loading parameter Δ. Values of energy function at $M + 1/2$ show energy needed to bring bond M to snapping point. Computations use Eqs. (26) and (29) with $N = 1000$ and $K = 512$ (see Appendix).

further. Figure 2 shows the energy of crack-line kinks as a function of length for many different values of Δ. The energies are calculated for integers and integers $+1/2$. For an integer l, the function shows the energy of an equilibrium kink configuration of length l, while for $l + 1/2$, the function shows the energy barrier separating the kink of length l from the kink of length $l + 1$. For $\Delta < 1.32$ a kink of length M must always surmount some energy barrier in order to become a kink of length $M + 1$, no matter how large M may be. For $\Delta > 1.32$ this statement is no longer true, and beyond some critical length M_c the kink will begin to run spontaneously along the crack like. At $\Delta \approx 1.63$ any kink longer than 1 atom wide runs spontaneously, and at $\Delta \approx 1.91$ the straight crack line is linearly unstable and begins to run all along its length at once.

In accord with the formalism of ref. 15, the probability of surmounting many energy barriers in sequence is the product of probabilities for surmounting the individual barriers. The total probability for a crack to advance a distance of one lattice spacing is therefore given by adding up all the activation energies in the corrugated function of Fig. 2. Figure 3 gives the total activation energy $E_{\text{tot}}(\Delta)$ computed in this way for crack advance as a function of Δ.

Because for $\Delta < 1.32$ kinks of all lengths have to surmount energy barriers in order to elongate, the activation energy is proportional to system width along m up to $\Delta = 1.32$; in fact, the kink would grow in length at some slow rate produced by thermal fluctuations, and the wider the sample along m, the slower the net motion of the crack along l. Making a definite prediction in this regime is tricky. If one picks any given system

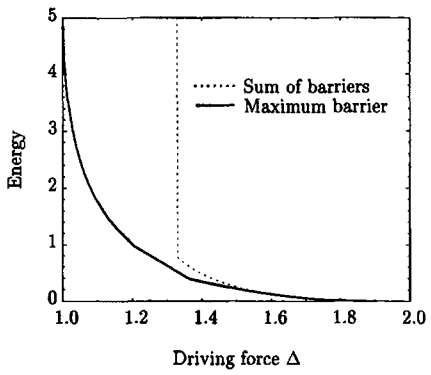

Fig. 3. Energy barriers to overcome in sending crack line ahead one lattice spacing. Solid like shows maximum energy that must be achieved, while dashed line shows sum of all upwards-moving parts of the energy surface. Computations using $N = 1000$, and $K = 512$ (see Appendix). Energy to break one bond is 2.

size and sends temperature to zero, then the most likely way for the crack to creep forward is by the motion of a single kink. However, if one picks any given low temperature and makes the system arbitrarily large then the most likely way for the crack to creep forward will involve multiple kinks forming simultaneously at exponentially large separations. In any event, the prediction of such large activation energies is almost certainly incorrect and arises because attention has been restricted to configurations of the transition state type. The crack can probably find a better way to advance by making a transition to a dynamical state where the kink runs at a rate on the order of the sound speed, rather than by waiting for a huge number of small thermal fluctuations to take it over barriers one at a time. This hypothesis should be checked with the general formalism of ref. 15, but will involve a very large numerical computation that has not been carried out. However, these ideas can be taken into account in a approximate way by assuming that once a crack rounds the top of one of the corrugated curves in Fig. 2 it will find a way to tumble over the remaining small barriers without further hindrance. In that case, the relevant energy barrier would be the highest point on each curve in Fig. 2. This quantity is also plotted in Fig. 3.

Once Δ exceeds 1.32, the total activation energy is found to be finite, and drops rapidly. By the time Δ has reached 1.5, the total energy needed for a whole crack line to advance is only one-tenth the energy needed to break a single unstrained bond. This observation provides an explanation in principle for the molecular dynamics calculations showing that crack creep merges seamlessly with dynamic fracture at temperatures on the

order of 100 K. It is only suggestive. The true energy surface of atoms interacting with Stillinger-Weber potentials can numerically be analyzed in an identical fashion, but this task also has not yet been carried out.

2. MODEL

A very simple model of three-dimensional crack lines is provided by linking side-by-side many copies of a one-dimensional model of fracture, and has been depicted in Fig. 1. The dynamics of this one-dimensional model has been discussed quite extensively in ref. 14, and its statistical mechanics in ref. 15. Equilibrium solutions of many side-by-side copies must obey

$$\sum_{\vec{\delta}} [u_{\vec{R}+\vec{\delta}} - u_{\vec{R}}] + \frac{1}{N} [U_N - u_{\vec{R}}] - 2u_{\vec{R}}\theta(u_{\vec{R}} - 1) = 0 \tag{2}$$

Here $\vec{R} = (l, m)$ ranges over a two-dimensional square lattice, and $\vec{\delta}$ ranges over the four nearest-neighbor vectors $(1, 0)$, $(-1, 0)$, $(0, 1)$ and $(0, -1)$. The function $u_{\vec{R}}$ gives the height of a mass point at each lattice location. The parameter U_N provides the driving force for crack motion, since it pulls every mass point upwards, while the parameter N should be thought of as a large number roughly representing the ratio between the height of a macroscopic strip and a lattice spacing. The computations reported in this paper use $N = 1000$. The only nonlinearity in Eq. (2) is provided by the Heaviside θ function, which causes the bond between the mass at $u_{\vec{R}}$ and its mirror image at $-u_{\vec{R}}$ to snap when $u_{\vec{R}} > 1$. Other bonds are not allowed to snap in this model, no matter how long they become. The energy needed to snap a single bond is $1/2 \times \text{Force} \times \text{Distance} = 1/2 \times 2 \times 2 = 2$, while the energy stored per lattice site far ahead of the crack tip is $2U_N^2/(2N+1)$, the leading factor of 2 coming from the fact that both upper and lower halves of the system store energy. For this reason, the proper dimensionless measure of loading is

$$\Delta \equiv \frac{U_N}{\sqrt{2N+1}} \tag{3}$$

since just enough energy is stored per lattice site to snap bonds when $\Delta = 1$.

The great advantage of snapping-bond potentials is that nonlinear operators such as in Eq. (2) can be converted instantly into linear operators by choosing a particular crack geometry. Suppose one has a crack

configuration $\{u^0\}$ where $u^0_{\vec{R}} > 1$ for all $\vec{R} = (l, m)$ with $l < 0$, and $u^0_{\vec{R}} < 1$ for all $l \geqslant 0$, as in Fig. 1(A). Let

$$\theta_l = \begin{cases} 0 & \text{for } l < 0 \\ 1 & \text{for } l \geqslant 0 \end{cases} \tag{4}$$

For this geometry, any solution of Eq. (2) is a solution of the linear problem, expressed in Dirac notation,

$$\langle \vec{R}| \hat{L}^0 |u^0\rangle = -\frac{U_N}{N} \tag{5}$$

where

$$\hat{L}^0 = \sum_{\vec{\delta}} (|\vec{R} + \vec{\delta}\rangle\langle \vec{R}| - |\vec{R}\rangle\langle \vec{R}|) - \frac{1}{N}[1 + 2N\theta_l]\, |\vec{R}\rangle\langle \vec{R}| \tag{6}$$

3. GREEN'S FUNCTIONS

Thomson[3, 12] has emphasized the value of Green's functions in dealing with fracture problems, and they provide the main tool for all the analysis. The Green function for $\hat{L}^0$ satisfies

$$\hat{G}^0 \hat{L}^0 = -I \tag{7}$$

where I here means the identity operator. Once $\hat{G}^0$ has been found, then

$$u^0_{\vec{R}} = \langle \vec{R} \,|\, u^0\rangle = \sum_{\vec{R}'} \langle \vec{R}|\, \hat{G}^0\, |\vec{R}'\rangle \frac{U_N}{N} \tag{8}$$

The actual form of $\hat{G}^0$ is of no particular interest, and a description of how it may be computed is relegated to an Appendix.

The task in this article is to take configurations such as Eq. (8) and to begin selectively snapping extra bonds along the crack line. Finding an equilibrium solution after breaking the bond at $\vec{R}_1 = (0, 1)$ means solving the equilibrium problem

$$\langle \vec{R}|\, \hat{L}^1\, |u\rangle = -\frac{U_N}{N} \tag{9}$$

where

$$\hat{L}^1 = \hat{L}^0 + 2\, |\vec{R}_1\rangle\langle \vec{R}_1| \tag{10}$$

The perturbation added to $\hat{L}^0$ is just what is needed to snap the bond at $\vec{R}_1$. According to Dyson's equation, ref. 16, p. 98, the Green function for $\hat{L}^1$ is

$$\hat{G}^1 = \hat{G}^0 + \hat{G}^0 \hat{T}^1 \hat{G}^0 \tag{11}$$

with

$$\hat{T}^1 = \frac{2\,|\vec{R}_1\rangle\langle\vec{R}_1|}{1 - 2\langle\vec{R}_1|\,\hat{G}_0\,|\vec{R}_1\rangle} \tag{12}$$

When not just one but M bonds $\vec{R}_1 \cdots \vec{R}_M$ have been snapped, then

$$\hat{G}^M = \hat{G}^0 + \hat{G}^0 \hat{T}^M \hat{G}^0 \tag{13}$$

with

$$\hat{T}^M = \sum_{nn'=1}^{M} 2\,|\vec{R}_n\rangle [1 - \hat{H}^M]^{-1} \langle \vec{R}_{n'}| \tag{14}$$

and

$$\langle\vec{R}|\,\hat{H}^M\,|\vec{R}'\rangle = 2\langle\vec{R}|\,\hat{G}^0\,|\vec{R}'\rangle \tag{15}$$

with the matrix elements of $\hat{H}^M$ being restricted to the subspace spanned by $\vec{R}_1 \cdots \vec{R}_M$, and $[1 - \hat{H}^M]^{-1}$ the $M \times M$ matrix inverse computed in this same space. Equation (15) is the main formal result upon which subsequent computations are based.

The patterns of broken bonds of interest are those such as in Fig. 1; that is, a line of M broken bonds reaching from $(0, 1)$ to $(0, M)$. The stability of a solution of this type with M broken bonds is determined by using Eq. (15) to compute the displacement $u_{\vec{R}_0}$, $\vec{R}_0 = (0, 0)$. If $u_{\vec{R}_0} < 1$ while $u_{\vec{R}_m} > 1$ for $1 \leqslant m \leqslant M$, the solution is consistent and stable. If it turns out that $u_{\vec{R}_0} > 1$, then a kink with M broken bonds is not stable, and the kink must spontaneously extend moving the crack forward.

The location of mass points when M bonds have broken is therefore, according to Eq. (13), and the analogue of Eq. (8),

$$u_{\vec{R}} = \frac{U_N}{N} \sum_{\vec{R}'} \{\langle\vec{R}|\,\hat{G}^0\,|\vec{R}'\rangle + \langle\vec{R}|\,\hat{G}^0 \hat{T}^M \hat{G}^0\,|\vec{R}'\rangle\} \tag{16}$$

Some simplifications occur in computing $u_{\vec{R}_0}$, which is

$$u_{\vec{R}_0} = \frac{U_N}{N} \sum_{\vec{R}'} \left\{ \langle \vec{R}_0 | \hat{G}^0 | \vec{R}' \rangle + \sum_{\vec{R}_m = 1}^{M} \langle \vec{R}_0 | \hat{G}^0 \hat{T}^M | \vec{R}_m \rangle \langle \vec{R}_m | \hat{G}^0 | \vec{R}' \rangle \right\} \quad (17)$$

It is legitimate to insert $\sum_{\vec{R}_m=1}^{M} \vec{R}_m | \langle \vec{R}_m |$ as a complete set of states because $\hat{T}^M$ only has nonzero matrix elements within this set of states. The first term on the right of Eq. (17) is just u_0^0, the height of the masses right along the crack line for the straight crack. In addition, since $\hat{G}^0$ is translationally invariant along the m direction, it must also be true that

$$\sum_{\vec{R}'} \frac{U_N}{N} \langle \vec{R}_m | \hat{G}^0 | \vec{R}' \rangle = u_0^0 \quad (18)$$

since $\vec{R}_m$ lies somewhere along the crack line. Therefore

$$u_{\vec{R}_0} = u_0^0 \left\{ 1 + \sum_{\vec{R}_m = 1}^{M} \langle \vec{R}_0 | \hat{G}^0 \hat{T}^M | \vec{R}_m \rangle \right\} \quad (19)$$

The condition for a kink of M broken bonds to be stable against further extension is therefore

$$\Delta < \frac{1}{[u_0^0/\Delta]\{1 + \sum_{\vec{R}_m=1}^{M} \langle \vec{R}_0 | \hat{G}^0 \hat{T}^M | \vec{R}_m \rangle\}} \quad (20)$$

Written in this fashion, it looks as if Δ should just cancel on both sides of Eq. (20), but remember that the driving force Δ is proportional to U_N, and that all the displacements $u_{\vec{R}}$ are proportional to U_N and hence Δ. For this reason $[u_0^0/\Delta]$ is a constant, independent of Δ, and Eq. (20) properly reports the upper load under which a kink is stable.

4. COMPUTING ENERGIES

Having determined the locations of all the mass points when various numbers of bonds have been snapped, it is next necessary to find the energies of the configurations. Given $u_{\vec{R}}$, and remembering that every point $u_{\vec{R}}$ has a mirror image at $-u_{\vec{R}}$ the energy is

$$E = \sum_{\vec{R}} 2 \left\{ \sum_{\vec{\delta}} \frac{1}{2} u_{\vec{R}} [u_{\vec{R}} - u_{\vec{R}+\delta}] + \frac{1}{2N} [U_N - u_{\vec{R}}]^2 \right\}$$
$$+ \frac{1}{2} [(2u_{\vec{R}})^2 \theta(1 - u_{\vec{R}}) + 4\theta(u_{\vec{R}} - 1)] \quad (21)$$

Multiplying Eq. (2) by $u_{\vec{R}}$ and summing over $\vec{R}$ allows Eq. (21) to be rewritten in the simpler form

$$E=\sum_{\vec{R}} \frac{U_N}{N}[U_N-u_{\vec{R}}]+2\theta(u_{\vec{R}}-1) \tag{22}$$

there is a first term that vanishes when each $u_{\vec{R}}$ relaxes to the equilibrium position U_N, and a second that counts the number of broken bonds. The difference in energy between a crack line with M extra broken bonds and a straight crack line is

$$\delta E=2M-\sum_{\vec{R}} \frac{U_N}{N}\delta u_{\vec{R}} \tag{23}$$

where $\delta u_{\vec{R}}$ is the change in location of mass points between the two configurations. To determine $\delta u_{\vec{R}}$, note that the first term on the right hand side of Eq. (16) is just $u^0_{\vec{R}}$, the configuration of a straight crack, and the remaining term must be $\delta u_{\vec{R}}$. Therefore

$$\delta E=2M-\left(\frac{U_N}{N}\right)^2 \sum_{\vec{R}\vec{R}'} \langle \vec{R}|\, \hat{G}^0\hat{T}^M\hat{G}^0\,|\vec{R}'\rangle \tag{24}$$

$$=2M-\left(\frac{U_N}{N}\right)^2 \sum_{\vec{R}\vec{R}'} \sum_{\vec{R}_{m'}=1}^{M} \langle \vec{R}|\, \hat{G}^0\,|\vec{R}_m\rangle\langle \vec{R}_m|\, \hat{T}^M\,|\vec{R}_{m'}\rangle\langle \vec{R}_{m'}|\, \hat{G}^0\,|\vec{R}'\rangle \tag{25}$$

$$=2M-\Delta^2\left(\frac{u_0^0}{\Delta}\right)^2 \sum_{\vec{R}_m\vec{R}_{m'}=1}^{M} \langle \vec{R}_m|\, \hat{T}^M\,|\vec{R}_{m'}\rangle \tag{26}$$

To obtain Eq. (26), make use of Eq. (18).

One final computation is needed. In order for a kink of length $M-1$ to turn into a kink of length M, the bond at $\vec{R}=(0, M)$ must be broken. There is a transition state involved in the breaking process if one considers that the force on the mass point does not pass immediately to zero when $u_{\vec{R}_M}$ reaches 1, but passes continuously but rapidly as $u_{\vec{R}_M}$ passes 1. As the force drops, there exists some value F_M between 0 and 2 for which the system is in unstable equilibrium with the bond poised on the edge of breaking. A solution of this type is obtained by returning to Eq. (16) and writing

$$u_{\vec{R}}=\sum_{\vec{R}'} \{\langle \vec{R}|\, \hat{G}^0\,|\vec{R}'\rangle+\langle \vec{R}|\, \hat{G}^0\hat{T}^{M-1}\hat{G}^0\,|\vec{R}'\rangle\}\left[\frac{U_N}{N}+F_M\,\delta_{\vec{R}',\vec{R}_M}\right] \tag{27}$$

The force F_M needs to be chosen so that $u_{\vec{R}_M} = 1$, since this bond is raised just to the breaking point. Let $\tilde{u}_M$ be the equilibrium height of the mass point at $\vec{R}_M$ when $M-1$ bonds have been broken. It must always be less than 1 for a stable kink. Then

$$F_M = \frac{1-\tilde{u}_M}{\langle \vec{R}_M | \hat{G}^0 | \vec{R}_M \rangle + \langle \vec{R}_M | \hat{G}^0 \hat{T}^{M-1} \hat{G}^0 | \vec{R}_M \rangle} \tag{28}$$

Finally, the extra energy needed in raising the force at $\vec{R}_M$ from zero to F_M so as to drag the mass point from $\tilde{u}_M$ to 1 is

$$\delta\tilde{E} = 2 \times \frac{1}{2} \frac{(1-\tilde{u}_M)^2}{\langle \vec{R}_M | \hat{G}^0 | \vec{R}_M \rangle + \langle \vec{R}_M | \hat{G}^0 \hat{T}^{M-1} \hat{G}^0 | \vec{R}_M \rangle} \tag{29}$$

the leading factor of two accounts for the energy needed to move the mirror image at $-u_{\vec{R}_M}$ downwards.

The energy surfaces in Fig. 2 were produced by using Eq. (26) to find the energies of equilibrium kink configurations of length M and plotting them at position M, then adding the extra energy given by Eq. (29) to see how much more energy was required to surmount the barrier leading to a kink of length $M+1$, and plotting this barrier energy at $M+1/2$.

APPENDIX: COMPUTATION OF $\hat{G}^0$

Consider a system that is infinite in the l direction, and periodic in the m direction, with period K. For a straight crack, the equations are independent of m, so it is profitable to Fourier transform the operator $\hat{L}^0$ in the m direction. Let

$$|m\rangle = \frac{1}{\sqrt{K}} \sum_{k=1}^{K} e^{2\pi i k m/K} |k\rangle \tag{30}$$

Then

$$\hat{L}^0 = \sum_k |k\rangle\langle k| \Big[(|l+1\rangle + |l-1\rangle - 2|l\rangle)\langle l| - \left(\frac{1}{N} + 2(1-\cos 2\pi k/K) + 2\theta_l\right) |l\rangle\langle l| \Big] \tag{31}$$

Since L^0 is diagonal in the k basis, the problem is reduced to finding the inverse of a one-dimensional operator depending on l. The equation that needs to be solved is

$$G^k_{l',l+1} + G^k_{l',l-1} - \left(\frac{1}{N} + 2 + 2\theta_l + 2(1-\cos 2\pi k/K)\right) G^k_{l',l} = -\delta_{l,l'} \quad (32)$$

Let

$$D = 2 + 1/N + 2(1-\cos 2\pi k/K), \qquad E = 4 + 1/N + 2(1-\cos 2\pi k/K) \quad (33)$$

$$0 = \alpha - D + \alpha^{-1}, \qquad 0 = \beta - E + \beta^{-1} \quad (34)$$

and let $\alpha_\pm$ and $\beta_\pm$ be the solutions of Eq. (34) with $\alpha_+ > 1$, $\alpha_- < 1$, and similarly for $\beta_\pm$.

The equations determining G^0 are

$l' > 0$:

$$G^k_{l,l'} = \begin{cases} A\beta_-^l & \text{for } l > l' \\ B_+\beta_+^l + B_-\beta_-^l & \text{for } 0 \leqslant l \leqslant l' \\ C\alpha_+^l & \text{for } l < 0 \end{cases} \quad (35)$$

The four unknown coefficients are determined by writing Eq. (32) out explicitly for $l = l'+1$, $l = l'$, $l = 0$, and $l = -1$, giving

$$\begin{pmatrix} 0 \\ -1 \\ 0 \\ 0 \end{pmatrix} = \begin{pmatrix} \beta_-^{l'+2} - E\beta_-^{l'+1} & \beta_+^{l'} & \beta_-^{l'} & 0 \\ \beta_-^{l'+1} & \beta_+^{l'-1} - E\beta_+^{l'} & \beta_-^{l'-1} - E\beta_-^{l'} & 0 \\ 0 & \beta_+ - E & \beta_- - E & \alpha_+^{-1} \\ 0 & 1 & 1 & \alpha_+^{-2} - D\alpha_+^{-1} \end{pmatrix} \times \begin{pmatrix} A \\ B_+ \\ B_- \\ C \end{pmatrix} \quad (36)$$

$l' = 0$, or $l' = -1$:

$$G^k_{l,l'} = \begin{cases} A\beta_-^l & \text{for } l \geqslant 0 \\ C\alpha_+^l & \text{for } l < 0 \end{cases} \quad (37)$$

Writing out Eq. (32) for $l = 0$ and $l = -1$ gives

$$\begin{pmatrix} -\delta_{l',0} \\ -\delta_{l',-1} \end{pmatrix} = \begin{pmatrix} \beta_- - E & \alpha_+^{-1} \\ 1 & \alpha_+^{-2} - D\alpha_+^{-1} \end{pmatrix} \begin{pmatrix} A \\ C \end{pmatrix} \quad (38)$$

$l' < -1$:

$$G^k_{l,l'} = \begin{cases} A\beta^l_- & \text{for } l > -1 \\ B_+\beta^l_+ + B_-\beta^l_- & \text{for } l' \leqslant l \leqslant -l \\ C\alpha^l_+ & \text{for } l < l' \end{cases} \tag{39}$$

Writing out Eq. (32) for $l=0$, $l=-1$, $l=l'$, and $l=l'-1$ gives

$$\begin{pmatrix} 0 \\ 0 \\ -1 \\ 0 \end{pmatrix} = \begin{pmatrix} \beta^1_- - E & \alpha^{-1}_+ & \alpha^{-1}_- & 0 \\ 1 & \alpha^{-2}_+ - D\alpha^{-1}_+ & \alpha^{-2}_- - D\alpha^{-1}_- & 0 \\ 0 & \alpha^{l'+1}_+ - D\alpha^{l'}_+ & \alpha^{l'+1}_- - D\alpha^{l'}_- & \alpha^{l'-1}_+ \\ 0 & \alpha^{l'}_+ & \alpha^{l'}_- & \alpha^{l'-2}_+ - D\alpha^{l'-1}_+ \end{pmatrix} \begin{pmatrix} A \\ B_+ \\ B_- \\ C \end{pmatrix} \tag{40}$$

Once $G^k_{l,l'}$ has been found, $\hat{G}^0$ is computed from

$$\langle m, l | \hat{G}^0 | m' l' \rangle = \sum_k \frac{1}{K} e^{-2\pi i k(m-m')/K} G^k_{l,l'} \tag{41}$$

Finally, it should be observed that the shape of the unperturbed crack, $u^0_{\bar{R}}$ is not most conveniently computed from Eq. (8), but instead may be found directly. The equation for it is

$$u^0_l = \begin{cases} \dfrac{U_N}{2N+1} + F\beta^l_- & \text{for } l \geqslant 0 \\ U_N + F'\alpha^m_+ & \text{for } l < 0 \end{cases} \tag{42}$$

with F and F' determined by

$$\frac{U_N}{2N+1} + F = U_N + F' \tag{43}$$

$$\frac{U_N}{2N+1} + F\beta^{-1}_- = U_N + F'\alpha^{-1}_+ \tag{44}$$

The figures in this paper were carried out with $K=512$ and $N=1000$.

ACKNOWLEDGMENTS

I would like to thank Leo Kadanoff for tolerating and even encouraging me during the time I began to learn about this subject, to thank Robb Thomson for asking the particular question from which this investigation

began, and to acknowledge support from the National Science Foundation, DMR-9531187, the Texas Advanced Research Program, the Exxon Education Foundation, and the U.S., Israel Binational Science Foundation, Grant 920-00148/1.

REFERENCES

1. D. Bensimon, L. P. Kadanoff, S. Liang, and B. I. Shraiman, Viscous flows in two dimensions, *Rev. Mod. Phys.* **58**:977–99 (1986).
2. R. Thomson, C. Hsieh, and V. Rana, Lattice trapping of fracture cracks, *J. Appl. Phys.* **42**(8):3154–3160 (1971).
3. R. Thomson, The physics of fracture, *Solid State Physics* **39**:1–129 (1986).
4. J. J. Gilman and H. C. Tong, Quantum tunneling as an elementary fracture process, *J. Appl. Phys.* **42**:3479-3486 (1971).
5. J. E. Sinclair, The influence of the interatomic force law and of kinks on the propagation of brittle cracks, *Philosophical Magazine* **31**:647–71 (1975).
6. A. S. Krausz and J. Mshana, The steady state fracture kinetics of crack front spreading, *Inter. J. Fract.* **19**:277–93 (1982).
7. I. H. Lin and J. P. Hirth, On brittle crack advance by double kink nucleation, *J. Mater. Sci.* **17**:447–60 (1982).
8. Sharad Ramanathan and Daniel S. Fisher, Dynamics and instabilities of planar tensile cracks in heterogeneous media, *Phys. Rev. Lett.* **79**:877–880 (1997).
9. C. Hsieh and R. Thomson, Lattice theory of fracture and crack creep, *J. Appl. Phys.* **44**:2051–2063 (1973).
10. B. R. Lawn, An atomistic model of kinetic crack growth in brittle solids, *J. Mater. Sci.* **10**:469–80 (1975).
11. A. J. Markworth and J. P. Hirth, An atomistic model of crack extension by kink propagation, *J. Mater. Sci.* **16**:3405–17 (1981).
12. R. Thomson, V. K. Tewary, and K. Masuda-Jindo, Theory of chemically induced kink formation on cracks in silica. I. 3-d crack Green's functions, *J. Mater. Res.* **2**:619–30 (1987).
13. D. Holland and M. Marder, Ideal brittle fracture of silicon studied with molecular dynamics, *Phys. Rev. Lett.* **80**:746–749 (1998).
14. M. Marder and S. P. Gross, Origin of crack tip instabilities, *J. Mech. Phys. Solids* **43**:1–48 (1995).
15. Michael Marder, Statistical mechanics of cracks, *Phys. Rev. E* **54**:3442–3454 (1996).
16. E. N. Economou, *Green's Functions in Quantum Physics* (Springer-Verlag, Berlin, 1983).